Supplementary Documentation

1. Remote Sensing Representations of Particle Size Distributions

It is very common in remote sensing aerosol models to assume that PSDs are superpositions of multiple modes, where each mode is approximated by a lognormal distribution (LND). Being lognormal, each mode is easily described by a normal distribution of the logarithm of the particle size ($l = lnD$):

$$n_l(l) = \frac{dN(l)}{dl} = \frac{dN(ln\ D)}{d\ (ln\ D)} = \frac{N_0}{\sqrt{2\pi}}\frac{1}{\sigma} exp\left[-\frac{(l-\mu)^2}{2\sigma^2}\right] \qquad \text{Eq 1.}$$

where N_0 is the total number of particles, defined as the integral of the number density distribution $n(l)$, and μ and σ are the mean and standard deviation of the log-diameter l, respectively. For simplicity, in the following we are considering distributions of spheroidal particles as that is what is assumed by most remote sensing algorithms. However, Saito and Yang (Saito 2022) have developed a generalized formula for interconverting PSDs of non-spherical particles. Notably they show that for non-spherical particles the size descriptor that gives consistent single scattering properties for different non-spherical shapes with the same size parameter is the effective radius.

One can write Eq 1 in linear diameter space by knowing that the mean log-diameter μ is equal to the natural logarithm of the median diameter $\widetilde{D}$ (i.e., $\mu = \ln \widetilde{D}$), and the log-diameter standard deviation σ is equal to the natural logarithm of the diameter geometric standard deviation S (i.e., $\sigma = \ln S$). Then Eq 1 becomes:

$$n(D) = \frac{N_0}{\sqrt{2\pi}}\frac{1}{\ln S}\frac{1}{D} exp\left[-\frac{\left(\ln D - \ln \widetilde{D}\right)^2}{2\,(\ln S)^2}\right] \qquad \text{Eq 2.}$$

This often leads to confusion among the aerosol community as some define standard deviation in terms of S (with values commonly between 1.5 and 2.0), whereas others define it in terms of σ (having values commonly between 0.4 and 0.7).

When it comes to computing *optical properties* for a given PSD, it is often most convenient to work with the nPSD. Scattering codes (Mie, T-Matrix, DDA, etc.) will compute extinction and scattering efficiencies (Q_{ext} and Q_{sca}) as a function of size parameter x for a given complex refractive index. The extinction and scattering efficiencies are convolved with the cross-sectional area distribution ($a(D)$) of the particle to derive the total extinction (and scattering) coefficients for a PSD:

$$\beta_{ext}(\lambda) = \int_{D=0}^{D=\infty} Q_{ext}(\lambda, D) a(D) n(D) dD \quad \text{Eq 3.}$$

$$= \int_{D=0}^{D=\infty} \left(\frac{\pi}{4}\right) D^2 Q_{ext}(\lambda, D) n(D) dD$$

$$\beta_{sca}(\lambda) = \int_{D=0}^{D=\infty} Q_{sca}(\lambda, D) a(D) n(D) dD \quad \text{Eq 4.}$$

$$= \int_{D=0}^{D=\infty} \left(\frac{\pi}{4}\right) D^2 Q_{sca}(\lambda, D) n(D) dD$$

These can be normalized by the total number of particles (e.g., $N_0 = \int_{D=0}^{D=\infty} n(D) dD$), to yield the scattering or extinction of an effective "single" particle (e.g., $\dot{\beta}_{ext}$ or $\dot{\beta}_{sca}$). Likewise, one must similarly integrate over size to calculate the vector phase function $P(\lambda, \theta)$ and asymmetry parameter $g(\lambda)$.

Computational integration across the interval $D = [0, \infty]$ is generally unnecessary (and impossible), so we limit the range to $D = [D_{min}, D_{max}]$. Integration is replaced by summation across *J* bins, having middle diameters D_j and widths ΔD_j. Bin $j = 1$ has diameter D_{min} and bin $j = J$ is D_{max}. We calculate extinction coefficient by the summation:

$$\beta_{ext}(\lambda) = \sum_{j=1}^{J} w_j a(D_j) Q_{ext}(\lambda, D_j) \quad \text{Eq 5.}$$

where the weights w_j for each bin are computed via the lognormal formula:

$$w_j = \frac{N_0}{\sigma\sqrt{2\pi}} \frac{1}{D_j} exp\left[-\frac{\left(ln\ D_j - ln\ \widetilde{D}\right)^2}{2\sigma^2}\right] \Delta D_j \quad \text{Eq 6.}$$

Similar summations can derive scattering coefficient β_{sca}, $P(\lambda, \theta)$ or $g(\lambda)$. However, the intervals ΔD_j must be small enough and the size range wide enough to "sufficiently" capture the properties of the size distribution. In other words, one requires that the summation derives a total number concentration approximately equal to the full distribution, e.g.:

$$C_n = \sum_{j=1}^{J} w_j \approx \int_{D=0}^{D=\infty} n(D) dD = N_0 \quad \text{Eq 7.}$$

Because peaks of the area and volume distributions are often skewed to much larger diameters than the number distribution, one should also ensure that total area and volume summations are also approximately equal to the full distribution values:

$$C_a = \sum_{j=1}^{J} w_j a(D_j) \cancel{w_j \left(\frac{\pi}{4}\right) D^2} \approx A_0 \quad \text{and} \quad C_v = \sum_{j=1}^{J} w_j v(D_j) \cancel{w_j \left(\frac{4\pi}{3}\right) D^3} \approx V_0 \qquad \text{Eq 8.}$$

As noted in section 3, the GRASP code includes a database representing spheroids with a fixed axis ratio distribution. That database is calculated using a scattering code and assumptions originally published by Dubovik et al. (2006), which we denote here as the DSL code. The DSL scattering code nominally assumes that particles exist in 41 bins with size parameters (defined as $x = 2\pi\, r_{sph}/\lambda$, where r_{sph} is the radius of a sphere of equivalent volume) spanning the range $0.012 \le x \le 625$, regularly spaced by intervals of log-diameter $\Delta \ln x_j = 0.271618$. This size parameter range is sufficient for capturing extinction and scattering by particles in solar wavelengths 0.34 μm < λ < 2.5 μm. For most PSDs described in the literature, this size range and bin distribution is sufficient for capturing >99.9% of the number, area, and volume distributions. Unless otherwise noted, we assume that reported optical properties can be sufficiently computed with this approximate size range and bin-intervals.

We showed we can derive extinction/scattering properties for an effective "unit" particle (e.g., $\dot{\beta}_{ext}$ or $\dot{\beta}_{sca}$). From this, one can pick a value of total extinction and derive the number (or volume) of particles necessary to achieve that extinction. For example, we might want to determine the number (or volume) concentration of particles C_n (or C_v) that lead to unit extinction coefficient at a given wavelength (e.g., $\beta_{ext}(\lambda) = 1.0$).

As an example, if the FMF or $\eta_{\lambda,f}$ is the fraction of total extinction contributed by fine mode aerosol, then the fine and coarse mode extinctions are given by:

$$\beta_{ext,f} = \eta_{\lambda,f}\beta_{ext} = \sum_{j=1}^{J} w_{j,f}\, a(D_j) Q_{ext}(\lambda, D_j) \qquad \text{Eq 9.}$$

and

$$\beta_{ext,c} = (1 - \eta_{\lambda,f})\beta_{ext} = \sum_{j=1}^{J} w_{j,c}\, a(D_j) Q_{ext}(\lambda, D_j) \qquad \text{Eq 10.}$$

On the other hand, one could also determine the number concentrations of each fine and coarse modes $C_{n,i} = \sum_{j=1}^{J} w_{j,i}$ that lead to that total extinction, and then define the FMF in terms of the number distribution:

$$\eta_{n,f} = \frac{C_{n,f}}{(C_{n,f} + C_{n,c})} \qquad \text{Eq 11.}$$

FMF can be defined by volume as well, leading to modal volumes (or volume fraction times total volume) that lead to a given value of total extinction, e.g., $C_{v,i} = \sum_{j=1}^{J} w_{j,i} v(D_j)$.

Clearly, if there are more than two modes, the concept of FMF, and fine/coarse mode number/volume becomes more difficult to define. For example, while the MODIS and OMI remote sensing algorithms tend to assume two lognormal distributions, the MISR community expects a combination of three (a 'fine', 'medium', and 'coarse').

2. AERONET Ground-Based Sun Photometer

There are two primary operational modes for AERONET. There is 'sun mode', where the robot points directly at the sun, and 'sky mode' where the robot points in discrete locations along the sky, including the almucantar (circle with constant view angle equal to the solar zenith angle) and the principal plane. Direct sun measurements are made approximately every 15 minutes, and sky measurements at several key times throughout the day. The AERONET sun mode observation directly measures the water vapor total column (WV) from the 936 nm channel, and spectral AOD from the remaining channels. Note that except for the 936 nm band, the standard wavelength bands used for AERONET are 'window' bands with non-negligible, but correctable trace-gas absorption.

Note that the AERONET literature describes products in terms of radius, but for convenience here, we have converted to diameter. Primary parameters include a) lognormal total volume particle size distribution (vPSD) as $\frac{dV(ln\ D)}{dln\ D}$ in units of [μm3/μm2] for 22 logarithmically equidistant discrete bins in the range 0.1μm ≤ D_j ≤ 30μm with intervals $\Delta \ln D_j = 0.2717$, b) complex refractive index at chosen wavelengths ($n(\lambda) = m(\lambda) + ik(\lambda)$), and the c) fraction of spherical particles (*f*). Note that the total volume concentration represents the aerosols leading to the total extinction (e.g., total optical depth) observed in the column, e.g.,

$$C_v = \int_{D=0.1}^{D=30.0} \frac{dV(D)}{d\ ln\ \ D} d\ ln\ D \qquad \text{Eq 12.}$$

From these *total* parameters, the inversion derives additional microphysical and optical properties that represent radiatively consistent *fine* and *coarse* aerosol modes. As described in Dubovik et al. (2000), the inversion code finds the minimum value of the vPSD within the interval 0.878 < *D* < 1.984 μm. This minimum 'inflection' diameter D_{inf} is used to separate between fine and coarse mode particles. Using that separation, the code reports properties of combined modes that best approximate the optical properties of the original vPSD. Thus, for each mode (i = f, c, and t), AERONET reports the median volume diameter $\widetilde{D}_{v,i}$ the log-size standard deviation σ_i, the effective diameter $D_{e,i}$, and the total volume $C_{v,i}$.

From these calculations, additional optical properties are estimated for each mode and wavelength, including: intensity phase function at 83 scattering angles $F_{11}(\theta, \lambda)$, SSA ω(λ), and asymmetry parameter g(λ). AERONET also reports parameters representing fluxes and radiative effects. Note that the retrieved complex refractive index is assumed to be the same for both modes, and that it is constrained by $1.33 \leq m(\lambda) \leq 1.6$ and $0.0005 \leq k(\lambda) \leq 0.5$ for each wavelength.

Details of the inversion are presented in Dubovik et al. (2006; 2000), with the heart of the inversion being the same Dubovik et al. (2006) (DSL) scattering code used for handling spheres or spheroids within GRASP. For the AERONET retrieval, introduced by Dubovik et al. (2006), the AERONET sky mode retrieval assumes a distribution of spheroids with a specific distribution N(ε) of 25 axis ratios ε shown in **Error! Reference source not found.** (see Dubovik_25 values and Table S1 for specific values). By adding a fraction f (sphere fraction) of spherical-only particles (ε = 1.0) to the spheroids, the inversion leads to a satisfactory solution in almost any case. These assumptions are used for the current Version 3 dataset (Sinyuk et al., 2020).

ε	N(ε)	ε	N(ε)	ε	N(ε)	ε	N(ε)	ε	N(ε)
0.3349	0.066185	0.5283	0.05335	0.8333	0	1.3145	0	2.0736	0.05872
0.3669	0.065025	0.5787	0.0477625	0.9129	0	1.44	0.0403205	2.2715	0.06205
0.4019	0.063635	0.6339	0.042953	1	0	1.5774	0.042953	2.4883	0.063635
0.4403	0.06205	0.6944	0.0403205	1.0954	0	1.728	0.0477625	2.7258	0.065025
0.4823	0.05872	0.7607	0	1.2	0	1.8929	0.05335	2.986	0.066185

Table S1 Aspect ratio and number weighting for the 25-aspect ratio spheroid distribution of Dubovik et al., 2006, assumed for AERONET inversion and many of the satellite aerosol models described in this paper.

Sensor	MODIS		VIIRS	
Satellite(s)	Terra & Aqua		SNPP & NOAA20	
	Band	Wave	Band	Wave

Deep Blue	B8	0.41	M1	0.41
Dark Blue	B9	0.44	M2	0.44
Blue	B3	0.47	M3	0.49
Green	B4	0.55	M4	0.55
Red	B1	0.65	M5	0.67
NIR	B2	0.86	M6	0.86
SWIR1	B5	1.24	M8	1.24
SWIR2	B6	1.63	M10	1.60
SWIR3	B7	2.11	M11	2.26

Table S2. Relevant solar reflective wavelength bands and center wavelengths (in μm) for passive sensors used for DT, DB and MAIAC aerosol retrieval algorithms (not all bands are used for every algorithm). Note the slight shifts in similar wavelength bands between sensors, that impact assumptions of aerosol models (optical properties) used in retrievals. Also note that even bands on twin sensors (on two different satellites) may have sufficiently different Relative Sensor Response to impact aerosol models and other retrieval assumptions.

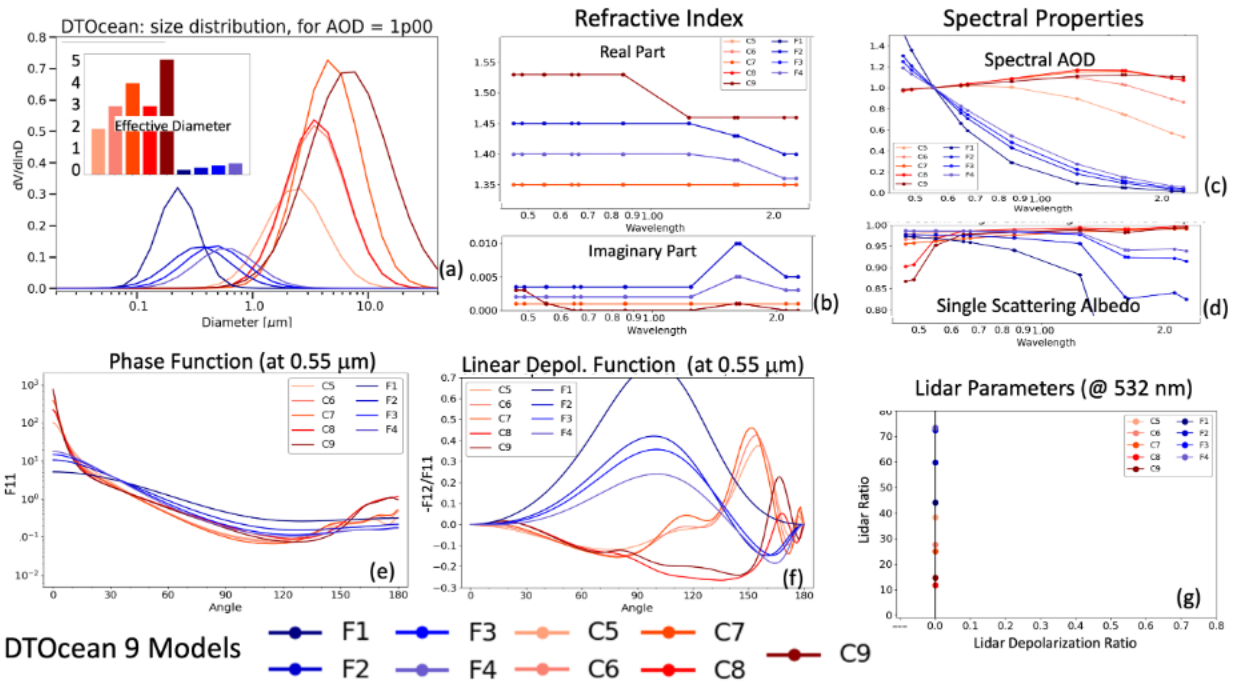

Figure S1. Physical and optical properties of the DT-Ocean 4 Fine (blue colors) and 5 Coarse Modes (red colors). (a) volume PSD for each mode with the effective diameter shown in inset, (b) spectral complex Refractive Index (c) spectral AOD, (d) spectral SSA, (e) phase function F11 at 0.55 m, (f) depolarization phase function $-F_{12}/F_{11}$ at 0.55 m, (g) lidar ratio versus lidar depolarization ratio at 532 nm. Note that the volume particle size distribution is normalized to represent a unit total extinction (e.g. AOD = 1.0) at 0.55 mm.

ε	N(ε)	ε	N(ε)
0.4019	0.14707	2.4883	0.16
0.4823	0.10779	2.0736	0.16848
0.5787	0.10779	1.728	0.14186
0.6944	0.06362	1.44	0.0906
0.8333	0	1.2	0
1	0		

Table S3 Aspect ratio and number weighting for the 11 aspect ratio distribution of Dubovik et al. (2002)

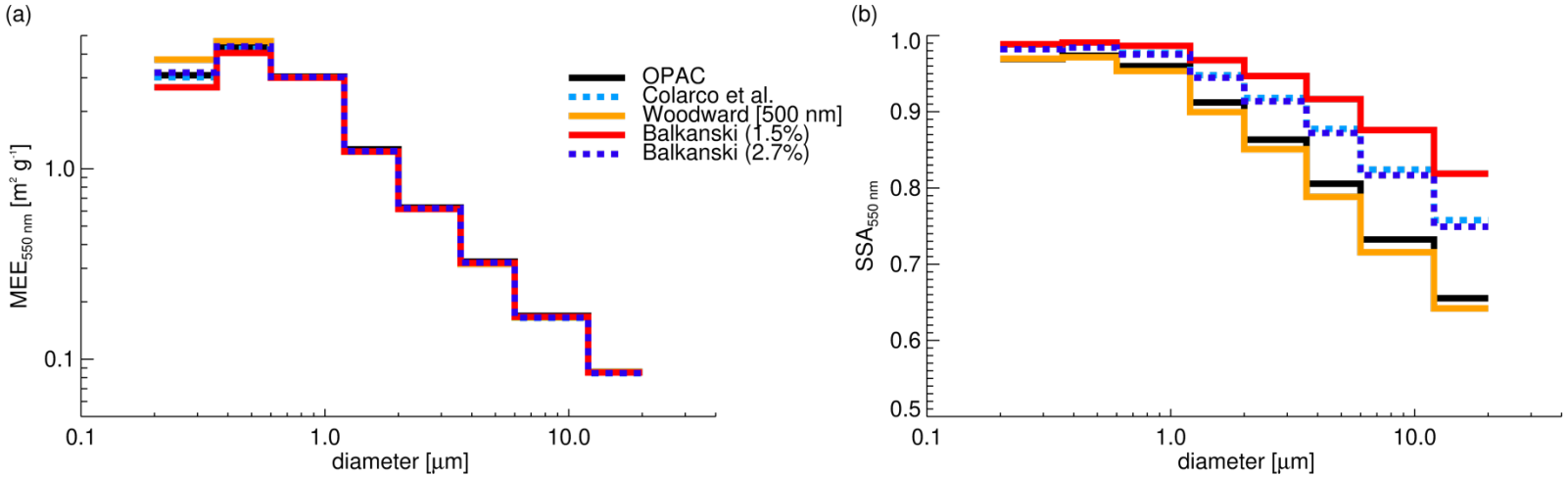

Figure S2. Similar to Figure 23 in Section 5 but for non-spherical optics.

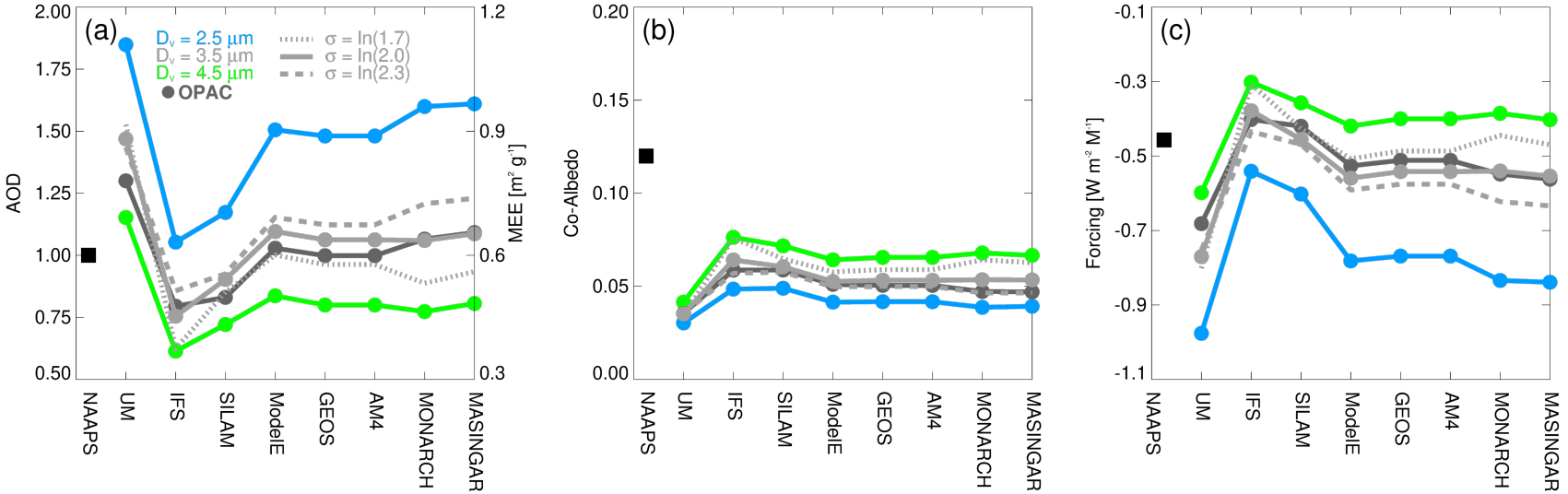

Figure S3. Similar to Figure 24 in Section 5 but for non-spherical optics.

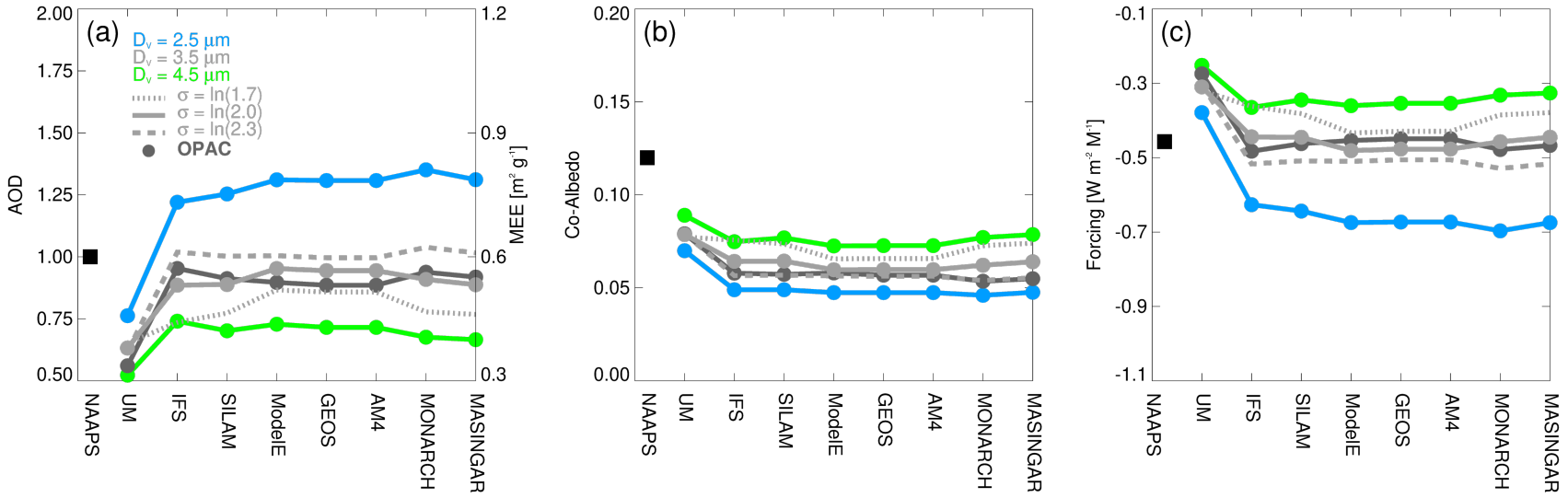

Figure S4. Similar to Figure 26 in Section 5 but for a sub-bin distribution described by $\widetilde{D_v}$= 3.5 µm and σ = ln(2.0).

REFERENCES

Dubovik, O., Holben, B., Eck, T.F., Smirnov, A., Kaufman, Y.J., King, M.D., Tanré, D., Slutsker, I., 2002. Variability of Absorption and Optical Properties of Key Aerosol Types Observed in Worldwide Locations. J Atmos Sci 59, 590–608. https://doi.org/10.1175/1520-0469(2002)059<;0590:voaaop>2.0.co;2

Dubovik, O., King, M.D., 2000. A flexible inversion algorithm for retrieval of aerosol optical properties from Sun and sky radiance measurements. J Geophys Res Atmospheres 105, 20673–20696. https://doi.org/10.1029/2000jd900282

Dubovik, O., Sinyuk, A., Lapyonok, T., Holben, B.N., Mishchenko, M., Yang, P., Eck, T.F., Volten, H., Muñoz, O., Veihelmann, B., Zande, W.J. van der, Leon, J., Sorokin, M., Slutsker, I., 2006. Application of spheroid models to account for aerosol particle nonsphericity in remote sensing of desert dust. J Geophys Res Atmospheres 1984 2012 111. https://doi.org/10.1029/2005jd006619

Sinyuk, A., Holben, B.N., Eck, T.F., Giles, D.M., Slutsker, I., Korkin, S., Schafer, J.S., Smirnov, A., Sorokin, M., Lyapustin, A., 2020. The AERONET Version 3 aerosol retrieval algorithm, associated uncertainties and comparisons to Version 2. Atmos Meas Tech 13, 3375–3411. https://doi.org/10.5194/amt-13-3375-2020